

Synthesis and Ink-Jet Printing of Highly Luminescing Silicon Nanoparticles for Printable Electronics

Anoop Gupta¹, Ahmed S. G. Khalil^{2,3}, Matthias Offer⁴, Martin Geller^{4,5},
Markus Winterer^{2,5}, Axel Lorke^{4,5}, and Hartmut Wiggers^{1,5,*}

¹*Institute for Combustion and Gasdynamics, University of Duisburg-Essen, Duisburg 47057, Germany*

²*Nanoparticle Process Technology, University of Duisburg-Essen, Duisburg 47057, Germany*

³*IBM Labs, 8803 Rüschlikon, Switzerland and Egypt Nanotechnology Center, El-Sheikh Zayed City, 12577 6 October & Fayoum University, 63514 Fayoum, Egypt*

⁴*Department of Physics, University of Duisburg-Essen, Duisburg 47057, Germany*

⁵*Center for NanoIntegration Duisburg-Essen (CeNIDE), University of Duisburg-Essen, Duisburg 47057, Germany*

Delivered by Ingenta to:

The formation of stable colloidal dispersions of silicon nanoparticles (Si-NPs) is essential for the manufacturing of silicon based electronic and optoelectronic devices using cost-effective printing technologies. However, the development of Si-NPs based printable electronics has so far been hampered by the lack of long-term stability, low production rate and poor optical properties of Si-NPs ink. In this paper, we synthesized Si-NPs in a gas phase microwave plasma reactor with very high production rate, which were later treated to form a stable colloidal dispersion. These particles can be readily dispersed in a variety of organic solvents and the dispersion is stable for months. The particles show excellent optical properties (quantum yields of about 15%) and long-term photoluminescence (PL) stability. The stable ink containing functionalized Si-NPs was successfully used to print structures on glass substrates by ink-jet printing. The homogeneity and uniformity of large-area printed film was investigated using photoluminescence (PL) mapping.

Keywords: Silicon, Nanoparticles, Photoluminescence, Ink-Jet Printing, Surface Functionalization.

1. INTRODUCTION

While high-tech devices are usually based on established technologies, an increasing interest in cost-effective alternatives in photovoltaics and optoelectronics is observed.¹ Silicon nanoparticles (Si-NPs) have become a significant material for large-area electronics because of potential applications that can benefit from the option to fabricate devices at low processing temperatures (<600 °C) and from the use of low cost substrates such as glass. Due to the larger optical band gap compared to relevant bulk silicon, Si-NPs are also interesting as an absorber layer in silicon and hybrid solar cell technology.

Over the past years, printing technology has attracted considerable attention due to simultaneous deposition and patterning of the different materials necessary to build the layers of an active device on any substrate, preferably without the need of a clean room or post-processing. Additionally, it enables new applications in the field of low cost printable electronic such as transistors,² solar cells³ and

full color displays.⁴ The current semiconductor fabrication technologies like photolithography are expensive and not feasible for large area processing, while technologies such as screen-printing and spin coating are not useful if the concentration of particle in the dispersion is very low. Additionally, these technologies need masks to write a well-defined pattern. Using ink-jet printing, the deposition of very small volume of suspensions in a well-defined pattern is possible and the direct structured deposition removes the need for masks leading to an efficient use of material. Moreover, ink-jet printing offers the deposition of nanoparticle dispersions with very low concentration due to the possibility of multilayer printing.

Ink-jet printing of different nanostructured materials such as Ag, Au, CdS and CdSe, nanoparticles has been successfully demonstrated in past.⁵⁻¹⁰ It has been shown that printed silver and gold nanoparticles could serve as conducting lines for electronic applications due to reasonably high conductivity.⁷⁻¹⁰ Loffredo et al.¹¹ have shown the ink-jet printing of polymer-carbon black composite film and its use as a chemical sensor. Mustonen et al.¹² demonstrated the controlled deposition of single-wall carbon

*Author to whom correspondence should be addressed.

nanotubes using ink-jet printing and observed a thickness-dependent conduction processes in printed films. From the point of view of cost, availability, non-toxicity and potential for integration into existing technologies, a high industrial demand exists on the use of Si-NP ink. However, the printing of Si-NPs has received little attention because of the lack of efficient routes to form stable silicon ink. To our knowledge, very few studies¹³ have been reported on the printing of Si-NPs and none was published using ink-jet printing.

Si-NPs usually tend to aggregate very easily, especially when dispersed in an organic medium. Liquid phase synthesis of Si-NPs in the presence of coordinating ligands has advantage in terms of instantly forming stable colloidal dispersion,¹⁴ however, these synthesis processes are disadvantageous in terms of low production rate. Unlike wet chemical routes, the plasma-assisted synthesis of Si-NPs ink offers the possibility of scale up the production but these particles do not show good optical properties.¹⁵ In this study, we present a facile method to produce large quantity of extremely stable Si-NPs ink with very good optical properties. We demonstrate that this stable Si-NP ink can be used to fabricate thin films on glass substrate using ink-jet printing. We also suggest an elegant tool to investigate the homogeneity and uniformity of large-area printed films using photoluminescence (PL) mapping.

2. EXPERIMENTAL DETAILS

We synthesized Si-NPs in a microwave plasma reactor by thermal decomposition of silane (SiH_4). This synthesis approach enables us to synthesize Si-NPs with very high production rates (up to 10 g h^{-1}).¹⁶ The Si-NPs with mean particle diameter of about 4.3 nm were examined in this study. The etching of the as-synthesized Si-NPs was carried out under inert conditions inside a glove box. In a typical experiment, 10 ml of HF acid (48 wt%) was added to a suspension of 50–60 mg Si-NPs in 5 ml of methanol. The dispersion was vigorously stirred for 30 min at room temperature and thereafter the particles were filtered on a polyvinylidene fluoride (PVDF) membrane filter (pore size $0.1 \mu\text{m}$). The functionalization of silicon surface was carried out with ethyl undecylenate using thermally induced hydrosilylation.¹⁷ For this purpose, freshly etched Si-NPs were transported into the ethyl undecylenate in an airtight glass bottle inside the glove box and the dispersion was heated to $120 \text{ }^\circ\text{C}$ for 10 h.

For ink-jet printing, a very low concentration of particles in the ink ($\sim 0.4 \text{ wt}\%$) was prepared with a viscosity of $2.3 \text{ mPa}\cdot\text{s}$. The viscosity of the ink was measured by a rheometer (Bohlin Gemini 150 from Malvern Instruments, UK) using plate-plate configuration at a temperature of $25 \text{ }^\circ\text{C}$ and a shear rate of 100 s^{-1} . A surface tension of $31 \text{ mN}\cdot\text{m}^{-1}$ was measured using a contact angle tool (DAS100, Krüss, Germany). The zeta potential as well as the particle size within the dispersion was

measured using a Zetasizer equipped with an autotitrator (ZetaNano, Malvern). Prior to printing, the glass substrates were cleaned in Piranha solution (3:1 volumetric mixture of sulfuric acid and hydrogen peroxide) for 30 min followed by rinsing several times in water and dried in a stream of dry nitrogen. A Dimatix 2800 ink-jet printer was used to print Si NPs on the cleaned glass substrates in a layer-by-layer fashion. The printing was carried out at 13 V and a frequency of 3 kHz. The substrate temperature was set at $60 \text{ }^\circ\text{C}$ and Si-NPs were printed on the glass substrate in a layer-by-layer fashion. There was a 10 min delay between two successively printed layers. The annealing treatment of the printed structure was carried out at $300 \text{ }^\circ\text{C}$ for 1 h. The thickness of the annealed Si-NPs films was measured using XP-200 profilometer (Ambios Technology).

The transmission electron microscopy (TEM) measurements on Si-NPs were performed using a Philips CM-20 operated at 200 kV. The surface chemistry of functionalized Si-NPs was investigated by Fourier transform infrared (FTIR) spectroscopy using a Bruker IFS66v/S spectrometer. For this purpose, the functionalized particles were separated from unreacted ethyl undecylenate by multiple centrifugations and measurement was done on dry particles in diffuse reflectance mode. The photoluminescence (PL) measurements were carried out at room temperature using a μ -PL setup with a Czerny-Turner monochromator (focal length $f = 500 \text{ mm}$). The sample was mounted on an x - y - z scanner and a diode-laser operated at $\lambda = 405 \text{ nm}$ was used as excitation source. On each scan position, a complete optical spectrum from 500 nm up to 850 nm was measured. All the photograph of luminescing Si-NPs were taken by exposing them to UV light ($\lambda = 366 \text{ nm}$). In order to measure the quantum yield of functionalized Si-NPs, the sample fluorescence was excited using a UV LED emitting at 390 nm and detected using a USB spectrometer from Ocean Optics (model USB200). The details of quantum yield measurement procedure is described elsewhere.¹⁸

3. RESULTS AND DISCUSSION

In previous communications,^{16,17} we have shown that the surface of our as-synthesized Si-NPs is covered with an oxide layer due to oxidation of particles in air. The etching of Si-NPs removes the oxide layer and terminates the surface with hydrogen. However, the oxide layer re-grows on the surface of etched Si-NPs upon exposure of particles in air. The functionalization of silicon surface with organic molecules via hydrosilylation process provides a promising route to stabilize their surface against air oxidation. Our previous study showed that ester-terminated Si-NPs exhibit higher stability in air compared to those which are bonded to alkyl groups.¹⁹ Additionally, the efficiency of surface functionalization of Si-NPs was found to be best with ethyl undecylenate compared to other commonly available esters. Therefore, in this study we functionalized the surface of Si-NPs with ethyl undecylenate.

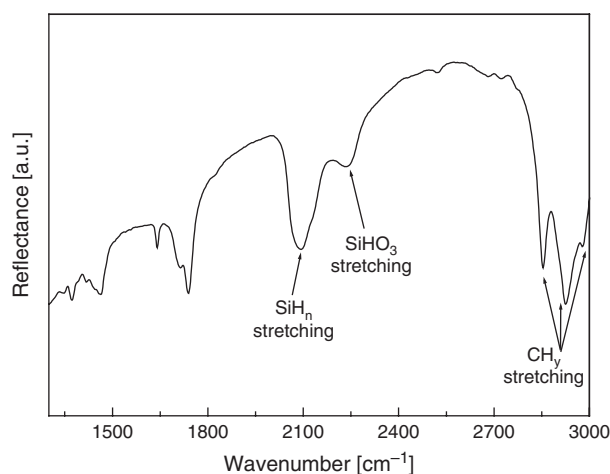


Fig. 1. FTIR spectrum of ethyl undecylenate functionalized Si-NPs.

Figure 1 shows the FTIR spectrum of Si-NPs functionalized with ethyl undecylenate. In the spectrum, sharp aliphatic CH_y stretching bands in the region of $3000\text{--}2855\text{ cm}^{-1}$ are present,²⁰ which originate from the attached ethyl undecylenate molecules on the silicon surface. Together with the characteristic peaks of ethyl undecylenate molecules, a small intensity of SiH_n ($n = 1, 2, 3$) stretching vibration around 2100 cm^{-1} can also be seen in the spectrum.²¹ This indicates that not all Si–H bonds on the silicon surface were replaced by alkyl groups because the initially attached alkyl groups on the silicon surface provide an increasing steric hindrance for further attachment of organic molecules. Additionally, a small peak around 2260 cm^{-1} appears in the spectrum, which can be assigned to Si–H stretching vibration in SiHO_3 configuration.²² It shows that etched particles also undergo

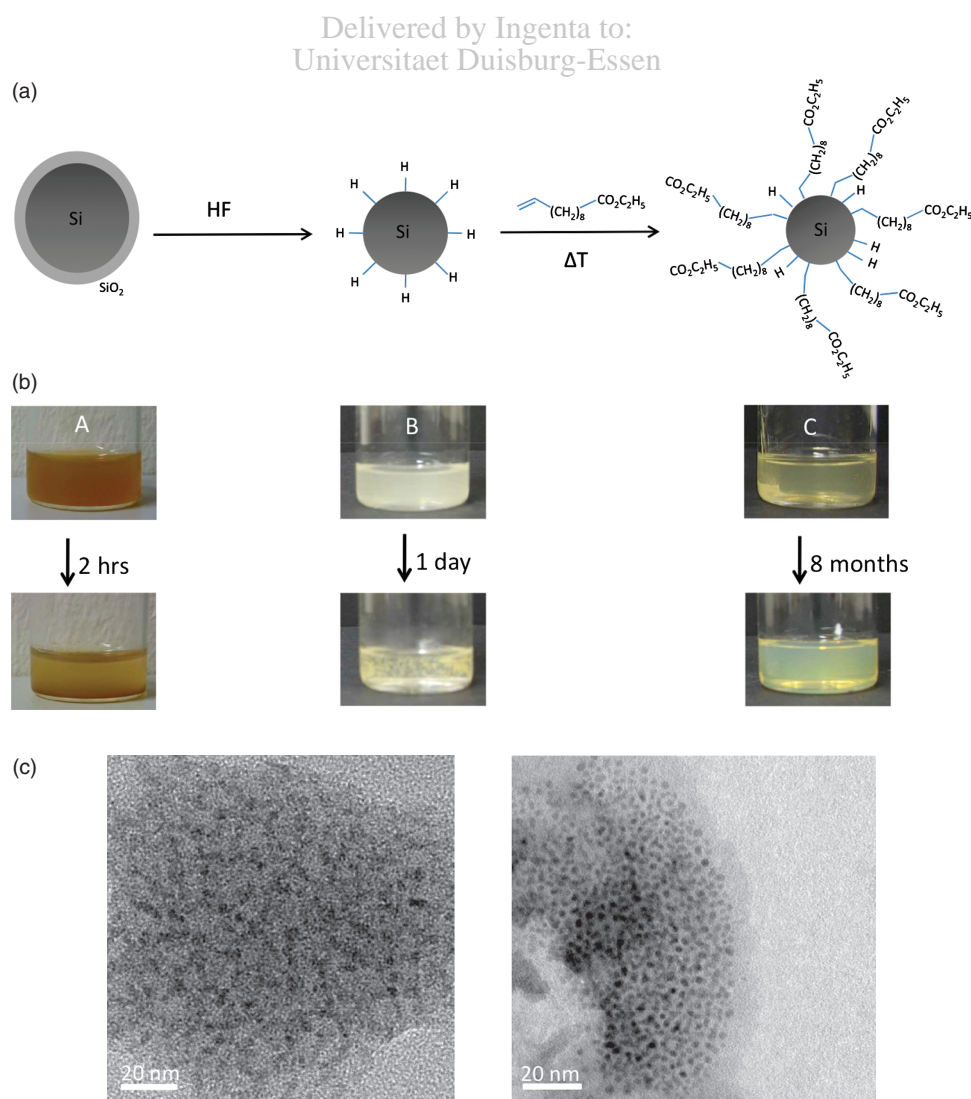


Fig. 2. (a) A schematic representation of etching and surface functionalization of Si-NPs with ethyl undecylenate molecules. (b) Photo of as-synthesized (sample A), freshly etched (sample B) and functionalized Si-NPs (sample C) dispersion in deionized water, chloroform and ethyl undecylenate solvent, respectively. (c) Bright field TEM image of as-synthesized (left) and functionalized Si-NPs (right).

some oxidation during the functionalization process, probably due to some traces of oxygen and moisture present in the reactants. We calculated the efficiency of functionalization to be 31%, which was determined from the ratio of change in integrated intensity of SiH_n vibration of functionalized sample over the original intensity.^{19, 23, 24}

Figures 2(a, b) shows a schematic representation of as-synthesized, freshly etched, and ethyl undecylenate functionalized Si-NP dispersions together with their dispersion stability in air under ambient conditions. It is observed that as-synthesized Si-NPs are very difficult to disperse because the particles are highly agglomerated (Fig. 2(c), left image) and the presence of an oxide shell around the Si-NPs limits the choice of a suitable dispersion medium. The dispersion of as-synthesized Si-NPs in de-ionized water is shown in Figure 2(b) (vial "A"). It is visibly turbid due to the presence of agglomerates and even ultrasonic treatment does not help to break the agglomerates. The average diameter of agglomerated, as-synthesized Si-NPs measured with dynamic light scattering was about 117 nm, which is about 28 times larger than their mean particle diameter. It is found that the zeta potential of the dispersion is not very high and therefore, a significant sedimentation of particles is observed after 2 hours. The etching of Si-NPs with HF acid removes the oxide layer and breaks the agglomeration of Si-NPs. However, it is found that the etched Si-NPs also do not form a stable dispersion in solvents because of re-oxidation and re-agglomeration of the particles.¹⁶ As an example, we show the dispersion stability of etched Si-NPs in chloroform (Fig. 2(b), vial "B"). A significant agglomeration of particle can be seen after 1 day of storage. The functionalization of freshly etched Si-NPs with organic molecules using hydrosilylation process provides passivation against surface re-oxidation. Additionally, the organic layer on the surface of Si-NPs provides steric hindrance for the further agglomeration of particles. The functionalized Si-NPs can be dispersed in organic solvent without any sonication due to presence of organic layer on their surface. In Figure 2(b) (vial "C"), the dispersion of functionalized Si-NPs in ethyl undecylenate solvent is shown. However, it is seen that after separating the functionalized Si-NPs from their respective alkenes, the particles can be re-dispersed in a variety of organic solvents (such as chloroform, toluene, *n*-hexane etc.) and the dispersion is extremely stable. The functionalized Si-NPs form an almost clear dispersion due to presence of non-agglomerated particles (Fig. 2(c)). The preservation of a non-polar particle surface provides better dispersability and long-term stability in organic solvents. The average diameter of functionalized Si-NPs measured using dynamic light scattering was about 28 nm, which is bigger than the mean particle diameter of as-synthesized Si-NPs due to the coating with organic molecules and probably some remaining agglomeration. We did not observe any reasonable change in hydrodynamic diameter of functionalized Si-NPs after 1 week

of storage, indicating that the dispersion is stable with time and no sedimentation of functionalized Si-NPs was observed even after months (visible inspection).

Si-NPs with diameter less than 5 nm show PL emission in the visible due to quantum confinement effects.^{25, 26} As a result, the functionalized particles prepared in this study show bright orange luminescence upon excitation with UV light (Fig. 3(a)). It is well known from the literature that the quantum yield (QY) of Si-NPs and porous silicon is very low. The QY of porous silicon was reported in the range of 1–10% for most of the samples.^{27, 28} Sankaran et al.²⁹ prepared blue luminescing Si-NPs and reported the QY of their particles of about 30%. Mangolini et al.³⁰ reported quantum yield of their functionalized Si-NPs

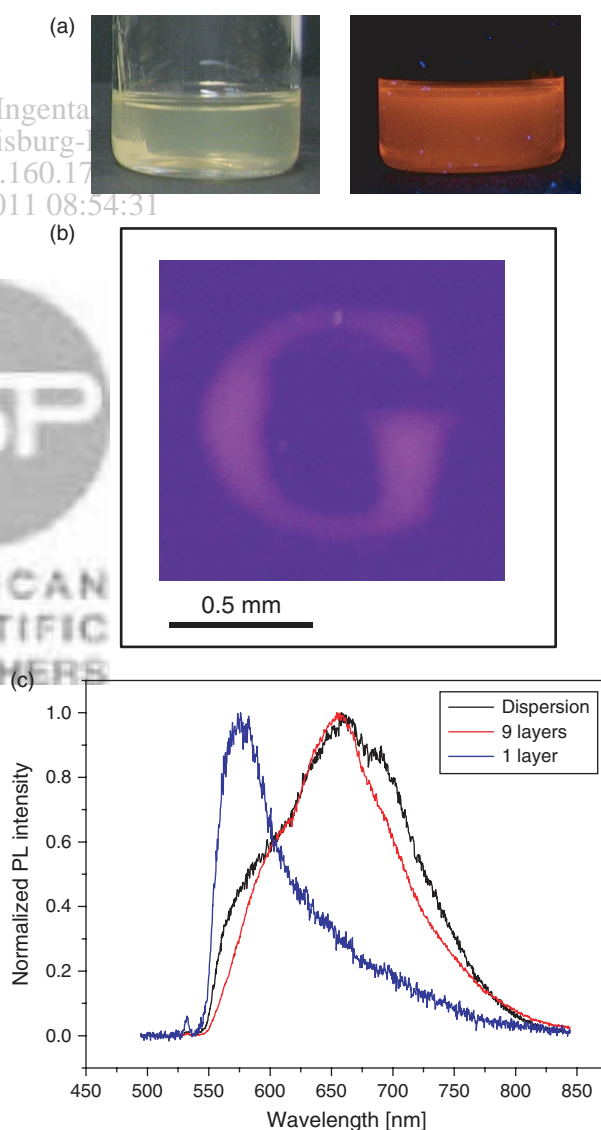


Fig. 3. (a) Functionalized Si-NPs dispersion in ethyl undecylenate under normal daylight and UV illumination. (b) Photograph of an ink-jet printed functionalized Si-NPs structure on glass substrate under UV illumination. (c) PL emission spectra from the dispersion, one ink-jet printed layer and nine ink-jet printed layers of functionalized Si-NPs.

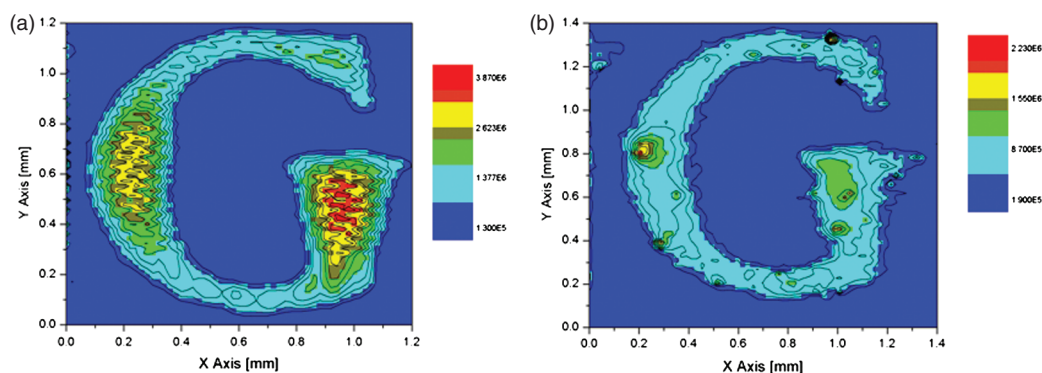


Fig. 4. Two dimensional intensity map of the printed structure “G” (a) before, and (b) after annealing.

maximum up to 70%. They also showed that the QY of Si-NPs decreases with the size of the NPs and their particles emitting below 700 nm show poor quantum yield (<5%). Our functionalized Si-NPs emit at around 660 nm and they still show a comparably high QY of about 15%. Additionally, these functionalized Si-NPs can be handled in air as the functional groups on the surface of Si-NPs provide passivation against oxidation. Moreover, these particles show stable luminescence for months.

As the dispersion of functionalized Si-NPs is very stable, it can be used to print structures on a substrate. The printing of functionalized Si-NPs was performed using ink-jet printing (see Experimental section for details). The printed structure was completely invisible to the unaided eye because of very high transparency of the printed thin film. However, when the printed structure was illuminated with UV light, the functionalized Si-NPs show visible luminescence. Figure 3(b) shows the picture of nine layers of a printed structure under UV illumination. The PL emission spectra recorded from the printed structure and from the dispersion are shown in Figure 3(c). After printing one layer, the structure shows an emission peak at 575 nm, however, the one with nine printed layers shows a strong red shift in the spectrum and emits at about 660 nm. We attribute this phenomenon to self-absorption within the emitting material.³¹ In case of nine printed layers, the photoluminescence from small nanoparticles that emit at shorter wavelength is suppressed due to the absorption from bigger particles, which then emit at higher wavelength. The probability of absorption of emission from small nanoparticles by big particles increases as it passes through many layers. Similarly in the PL spectrum of the dispersion, the emission from the small nanoparticles at about 575 nm is suppressed by big particles and therefore it shows a main peak around 660 nm and a shoulder at 575 nm.

The homogeneity and uniformity of printed Si-NPs films was analyzed by photoluminescence scanning. The structure “G” was scanned in two dimensions using intensity integration from 500 nm to 850 nm and a two-dimensional intensity map was created. With this inten-

sity mapping the concentration distribution of particles at different position in the printed structure was analyzed. Figure 4 shows the 2-D intensity profile of a printed structure “G” (consisting of nine layers) before and after annealing. The as-prepared structure did not show a homogenous distribution of particles over the entire structure as evidenced by a strong variation of the intensity within the pattern. The particles are mostly concentrated, where the structure is relatively wide. At a particular position, the concentration of particles is high at the center and decreases towards the edges. In addition to that the printed structure “G” has not well-defined edges. The inhomogeneity of the printed structure “G” is mainly due to the slow drying of the printed layers. For our experiments, the substrate was heated up to 60 °C, which is the maximum possible temperature of the substrate heater used. This temperature is very low compared to the evaporation temperature of our solvent (B.P. = 258 °C) so that the printed layers are still ‘wet’ even for longer delay times between the over printing. After annealing of the printed structures, the distribution of particles was more homogeneous due to evaporation of the solvent. The thickness of the annealed films was between 100–240 nm. It is known from the literature that the morphology of deposited particles depends on various factors, such as particles concentration and choice dispersion medium.³² Therefore, by optimizing these parameters, more homogeneous and well-defined pattern of Si-NPs can be obtained.

4. CONCLUSIONS

Using microwave plasma synthesis approach, a large quantity of highly stable Si-NPs inks can be produced. The as-synthesized Si-NPs do not easily form stable dispersion in solvents due to the presence of agglomerates and surface Oxides. The etching and functionalization of the nanoparticle surface break their agglomeration and terminate the surface with organic molecules. The presence of organic ligands on the surface of Si-NPs allows them to form very stable inks in a variety of organic solvents. The Si-NP inks

show very good optical property with long-term PL stability. It is shown that the dispersion of functionalized Si-NPs can be used to print structures on a substrate. PL mapping was used to analyze the homogeneity and optical quality of ink-jet printed layer.

Acknowledgments: Financial support of the German Research Foundation (DFG) through the Research Training Group 1240 (GRK 1240 Nanotronics—Photovoltaik und Optoelektronik aus Nanopartikeln) is greatly acknowledged. The authors are thankful to Ralf Theissmann for TEM measurements, and Ryan Gresback and Uwe Kortshagen for QY measurement.

References and Notes

1. C. J. Brabec, *Energy Mater. Solar Cells* 83, 273 (2004).
2. H. Sirringhaus, T. Kawase, R. H. Friend, T. Shimoda, M. Inbasekaran, W. Wu, and E. P. Woo, *Science* 290, 2123 (2000).
3. C. N. Hoth, S. A. Choulis, P. Schilinsky, and C. J. Brabec, *Adv. Mater.* 19, 3973 (2007).
4. V. Wood, M. J. Panzer, J. Chen, M. S. Bradley, J. E. Halpert, M. G. Bawendi, and V. Bulovic, *Adv. Mater.* 21, 2151 (2009).
5. H. H. Lee, K. S. Chou, and K. C. Huang, *Nanotech.* 16, 2436 (2005).
6. C. Ingrosso, J. Y. Kim, E. Binetti, V. Fakhfour, M. Striccoli, A. Agostiano, M. L. Curri, and J. Brugger, *Microelectron. Eng.* 86, 1124 (2009).
7. W. Cui, W. Lu, Y. Zhang, G. Lin, T. Wei, and L. Jiang, *Colloids Surf., A* 358, 35.
8. I.-K. Shim, Y. Lee, K. J. Lee, and J. Joung, *Mater. Chem. Phys.* 110, 316 (2008).
9. H.-W. Lin, W.-H. Hwu, and M.-D. Ger, *J. Mater. Process. Technol.* 206, 56 (2008).
10. H.-H. Lee, K.-S. Chou, and K.-C. Huang, *Nanotech.* 16, 2436 (2005).
11. F. Loffredo, A. D. G. D. Mauro, G. Burrasca, V. La Ferrara, L. Quercia, E. Massera, G. Di Francia, and D. D. Sala, *Sens. Actuators, B* 143, 421 (2009).
12. T. Mustonen, J. I. Mäklin, K. Kordás, N. Halonen, G. Tóth, S. I. Saukko, J. Vähäkangas, H. Jantunen, S. Kar, P. M. Ajayan, R. Vajtai, P. Helistö, H. Seppä, and H. Moilanen, *Phys. Rev. B* 77, 125430 (2008).
13. M. Harting, J. Zhang, D. R. Gamota, and D. T. Britton, *Appl. Phys. Lett.* 94, 193509 (2009).
14. J. P. Wilcoxon, G. A. Samara, and P. N. Provencio, *Phys. Rev. B* 60, 2704 (1999).
15. L. Mangolini and U. Kortshagen, *Adv. Mater.* 19, 2513 (2007).
16. A. Gupta, M. T. Swihart, and H. Wiggers, *Adv. Funct. Mater.* 19, 696 (2009).
17. A. Gupta and H. Wiggers, *Physica E* 41, 1010 (2009).
18. L. Mangolini, D. Jurbergs, E. Rogojina, and U. Kortshagen, *J. Lumin.* 121, 327 (2006).
19. A. Gupta, S. Kluge, C. Schulz, and H. Wiggers, *Mat. Res. Soc. Symp. Proc.* 1207, N02 (2010).
20. W. Simons (ed.), *The Sadtler Handbook of Infrared Spectra*, Heyden & Son, Philadelphia, PA (1978).
21. D. C. Marra, E. A. Edelberg, R. L. Naone, and E. S. Aydil, *J. Vac. Sci. Technol. A* 16, 3199 (1998).
22. M. Niwano, J.-I. Kageyama, K. Kurita, K. Kinashi, I. Takahashi, and N. Miyamoto, *J. Appl. Phys.* 76, 2157 (1994).
23. M. P. Stewart, E. G. Robins, T. W. Geders, M. J. Allen, H. C. Choi, and J. M. Buriak, *Phys. Status Solidi A* 182, 109 (2000).
24. J. Nelles, D. Sendor, A. Ebbers, F. Petrat, H. Wiggers, C. Schulz, and U. Simon, *Colloid Polym. Sci.* 285, 729 (2007).
25. G. Ledoux, O. Guillois, D. Porterat, C. Reynaud, F. Huisken, B. Kohn, and V. Paillard, *Phys. Rev. B* 62, 15942 (2000).
26. C. Meier, A. Gondorf, S. Lutjohann, A. Lorke, and H. Wiggers, *J. Appl. Phys.* 101, 103112 (2007).
27. W. L. Wilson, P. F. Szajowski, and L. E. Brus, *Science* 262, 1242 (1993).
28. L. Brus, *J. Phys. Chem.* 98, 3575 (1994).
29. R. M. Sankaran, D. Holunga, R. C. Flagan, and K. P. Giapis, *Nano Lett.* 5, 537 (2005).
30. L. Mangolini, D. Jurbergs, E. Rogojina, and U. Kortshagen, *Phys. Stat. Sol. (c)* 3, 3975 (2006).
31. R. Wang, J. Peng, F. Qiu, Y. Yang, and Z. Xie, *Chem. Commun.* 6723 (2009).
32. J. Park and J. Moon, *Langmuir* 22, 3506 (2006).

Received: 6 September 2010. Accepted: 17 December 2010.